The Astrophysical Journal, 890:170 (12pp), 2020 February 20 https://doi.org/10.3847/1538-4357/ab6ef4

Collisional Evolution of Meter- to Kilometer-sized Planetesimals in Mean Motion Resonances: Implications for Inward Planet Shepherding

Rogerio Deienno, Kevin J. Walsh, Harold F. Levison, and Katherine A. Kretke
Department of Space Studies, Southwest Research Institute, 1050 Walnut St., Boulder, CO 80302, USA; rdeienno@boulder.swri.edu
Received 2019 September 24; revised 2020 January 8; accepted 2020 January 21; published 2020 February 26

Abstract

Small particles (meter to kilometer sized) can drift inward through a protoplanetary disk owing to their interaction with a gaseous nebula. If planets exist, these particles can get captured in mean motion resonance (MMR) and, if massive, exchange angular momentum with the planets. While dependent on the total mass in small inward-drifting particles captured, the main result out of such resonant angular momentum exchange is inward planet shepherding. However, it is not clear what the real dynamics of a large number of massive particles in MMR would be when collisional effects are included. Therefore, we studied the capture mechanism and collisional evolution of a swarm of massive inward-drifting particles in MMRs with planets. Due to the confined space of an MMR, captured massive particles can rapidly collisionally evolve. Our main results show that, if massive particles are assumed to be rocky, collisions make the swarm of particles decrease in size. In this case, as their gas drag properties change (smaller particles drift faster through the gas nebula), they eventually leave the MMR. On the other hand, if massive particles are assumed to be 10, 100, or 1000 times stronger (harder to break) than rocky particles, they instead grow. In this situation, the drifting particles slow down ($r \gtrsim 1$–5 km) or even stop ($r \gtrsim 5$–10 km) their inward drift. We conclude that, although some angular momentum exchange may exist, in no cases studied here did the massive inward-drifting particles significantly change the orbit of the planet.

Unified Astronomy Thesaurus concepts: Planet formation (1241); Planetary system formation (1257); Dynamical evolution (421)

1. Introduction

Objects of different sizes interact differently with the gaseous component of a protoplanetary disk (Adachi et al. 1976). In the particular case of small, meter- to kilometer-sized particles, due to the differences between the Keplerian orbital velocities and the gas velocities (i.e., the gas nebula rotates slightly more slowly than the Keplerian velocity; Adachi et al. 1976), these particles experience orbital decay, resulting from loss of energy and angular momentum, along with eccentricity and inclination damping (Adachi et al. 1976; Weidenschilling 1977). Interested in whether the presence of planets could stop these inward-migrating particles from hitting the star, many authors studied the dynamical behavior of these objects near mean motion resonances (MMRs; Weidenschilling & Davis 1985; Patterson 1987; Beauge & Ferraz-Mello 1993; Malhotra 1993a; Gomes 1995a, 1995b; Jiang & Yeh 2004, to cite a few). Most of these works are related to resonance trapping exterior to the orbit of the planet. It was found that the capture of inward-drifting particles, although efficient at times, is still a probabilistic event. There is a strong relationship with the size of the particles—which, together with gas disk parameters and distance from the star, determine how fast the particles drift inward—and the strength of each MMR crossed, which is related to the mass of the planet. It had been demonstrated that inward-drifting particles can preferentially be captured if they approach a given MMR with certain orbital conditions, i.e., with eccentricities of the order of or larger than a specific value of equilibrium eccentricity (Section 3, Equation (1)), or if they drift slow enough in order to have their eccentricity pumped up to such equilibrium eccentricity during the MMR crossing (Beauge & Ferraz-Mello 1993; Malhotra 1993a; Gomes 1995a, 1995b). This is a relevant result for the present study, especially because this work is focused on the dynamical evolution of inward-drifting particles captured in MMR. For this reason, we are going to dedicate a section in the present work to reassessing and showing this mechanism (see Section 3).

Capture of inward-drifting planetesimals in exterior MMRs has been found to be important in studies of giant planet core formation (Levison et al. 2010). One outstanding feature observed by Levison et al. (2010, see Figure 6 in their work) was that, given the generous amount of mass within small inward-drifting planetesimals' fragments trapped in MMR, the giant planets' cores can be shepherded inward. This happens because small fragments can drift inward very fast in the gaseous disk, and when trapped in MMR, this fast inward drift is stopped, causing the orbital eccentricity of the small fragments to grow. However, due to the fact that the interaction of the fragments with the gas still exists, larger fragments' eccentricities imply more angular momentum loss and faster inward-drifting rates (Weidenschilling & Davis 1985; Levison et al. 2010). When locked in resonance, this results in a shared angular momentum loss with the interior planet. Levison et al. (2010) even found extreme cases where planets were pushed into the star.

Similarly, Batygin & Laughlin (2015) proposed that a full system of planets like Keppler-11 (Lissauer et al. 2011) could be pushed into the host star under specific conditions. Within the solar system view, assuming the minimum-mass solar nebula prescription (Weidenschilling 1977; Hayashi 1981), Batygin & Laughlin (2015) computed that if 20 $M_\oplus$ (where $M_\oplus$ stands for Earth mass) of inward-drifting planetesimals composed by $r = 100$ m objects get trapped in MMR with the outermost planet, a system of super-Earths could be pushed into their star. Therefore, Batygin & Laughlin (2015) concluded that the lack of super-Earths with orbits interior to

that of Mercury in our solar system could be a by-product of the occurrence of the Grand Tack model (Walsh et al. 2011). Even when gravitational interaction among planetesimals is considered, the results by Batygin & Laughlin (2015) hold (Storch & Batygin 2019); however, in this scenario some planetesimals can be lost, i.e., escape from the MMR in which they were captured, due to gravitational interaction, and then, because they continue drifting inward, leave the system by either accreting into the planet or into the star.

Although the likelihood of planets falling, or being pushed, into the host star can be put into question (see Masset et al. 2006 and associated discussion regarding planet traps in Morbidelli et al. 2016), the fact that Levison et al. (2010), Batygin & Laughlin (2015), and Storch & Batygin (2019) reported planet inward shepherding by planetesimal swarm is intriguing by itself.

One important aspect, though, as anticipated in Weidenschilling & Davis (1985) and briefly discussed in Levison et al. (2010), is that the induced eccentricities of the particles when in MMRs can be large. This will result in the overlap of orbits for bodies inside a single MMR or even in different close resonances, as well as with nonresonant objects, and possibly with larger objects in the disk as well. This could lead the captured objects to leave the MMR by either being kicked out of the resonance or collisionally evolving (especially considering the huge density that these small objects can represent when piled up within a narrow resonant region).

Marzari & Weidenschilling (2002) reported that, under the influence of Jupiter, planetesimals have their eccentricities excited during resonance crossing, but keeping low inclination, therefore implying significant collisional evolution during migration within a gaseous disk. Similarly, Chrenko & Broz (2015) found that planetesimals captured by a Jovian planet in an interior MMR tend to have their eccentricity increased, overcoming the damping effect from the gas nebula. This would then lead these planetesimals trapped in MMR to cross orbits with other planetesimals within the disk. More recently, Wallace et al. (2019) also found that, in a gaseous environment, planetesimals within MMR under the gravitational influence of an external Jupiter-sized planet tend to have their collision rate interior to the nominal resonance locations enhanced, increasing dust production. These results support the predictions by Weidenschilling & Davis (1985), discussed in the previous paragraph, and serve as motivation for the present study.

Therefore, in this work we devote our attention to closely studying the collisional evolution of a massive, gravitationally interacting, inward-drifting swarm of small (meter- to kilometer-sized) planetesimals trapped in MMRs with an interior planet. The goal of our work is to determine whether the inward planet shepherding process by MMR holds when the massive inward-drifting planetesimals gravitationally interact, and when collisions and fragmentation are allowed to occur. This way, the present work has the important task of validating or invalidating such an inward planet shepherding mechanism.

This paper is structured as follows. In Section 2 we describe our code setup. In Section 3 we give a brief review of the capture mechanism of inward-drifting planetesimals by an existing planet, highlighting the main features. Section 4 is devoted to simulations with and without collisional evolution. In this section we present all of our results—without collisional evolution (Section 4.1) and with collisional evolution (Sections 4.2.1–4.2.3). Section 5 concludes the paper.

2. The Code

Regarding the capture and evolution of small inward-drifting particles within MMRs, all works discussed in the previous section considered either massless test particles or massive but noninteracting planetesimals (the exception is Storch & Batygin 2019; however, they do not address the capture mechanism). The works that considered massive inward-drifting planetesimals, due to computational limitations, only assumed a small number of planetesimals with large masses.

In this work, in order to consider a large number of massive inward-drifting planetesimals that can gravitationally interact and also collisionally evolve, we use the code known as LIPAD (Levison et al. 2012). LIPAD uses the concept of Lagrangian particles, known as "tracers," to track the evolution of a large number of planetesimals with a given radius and similar orbits. As described in Levison et al. (2012), the number of planetesimals that a single tracer represents is defined by $n_{\rm pl} = m_{\rm tr}/[(4/3)\pi\rho r_{\rm pl}^3]$, where $m_{\rm tr}$ is the mass of the tracer (constant), ρ the planetesimal bulk density, and $r_{\rm pl}$ the radii of the planetesimals represented by that tracer. The mass of each planetesimal inside one tracer is $m_{\rm pl} = m_{\rm tr}/n_{\rm pl}$. In this work we will always consider a bulk density of $3\,{\rm g\,cm^{-3}}$ for the planetesimals. Due to the fact that $n_{\rm pl}$ is a real number, if the number of planetesimals inside a tracer is smaller than or equal to unity, LIPAD assumes $n_{\rm pl} = 1$ and $m_{\rm pl} = m_{\rm tr}$.

Within the scope of this work tracer particles interact with embryos via direct N-body (SyMBA; Duncan et al. 1998) routines (here "embryos" represent classical N-body massive particles and are represented by the planets in our work—we highly encourage the reader to refer to Levison et al. 2012 for a complete description of different object classes and their interaction, as not all of the LIPAD component interactions are relevant for the present work). Also, the planetesimals inside a single tracer, as well as inside different tracers, may or may not (this is a decision of the user) have gravitational interactions with each other and also may or may not collisionally evolve through statistical routines throughout the simulation. This means that, when gravitational interactions and collisions are allowed, all planetesimals (within all tracers) in the simulation do gravitationally interact and collisionally evolve through statistical routines. In other words, although many planetesimals are represented by a considerably smaller number of tracers, collisions and gravitational interaction happen among planetesimals. In the case where collisional evolution is allowed, when a collision between planetesimals happens, the size of the largest remnant, the number of fragments, and the size frequency distribution (SFD) resulting from such a collision are determined by the Benz & Asphaug (1999) fragmentation law. From this SFD new radii for the surviving planetesimals are selected probabilistically such that over the large numbers of collisions among large numbers of planetesimals in a given region of the simulation, characteristic SFDs are well represented (see Levison et al. 2012, for more specific details on the statistics for collisions). Therefore, as a tracer represents several planetesimals of similar sizes, the radii of the tracers in the nearby location of the collision can change (be rearranged) to represent the swarm of fragments generated, thereby representing all radii ($r_{\rm pl}$) of the planetesimals' SFD. In this sense, the radius of a tracer can either decrease (representing a larger number of small planetesimals) or increase (representing a smaller number of large planetesimals). The total mass, radius, and number of planetesimals inside a

given tracer will be reported for each different simulation performed in this work.

LIPAD also has a prescription of the gaseous nebula from Hayashi et al. (1985). This gas disk provides aerodynamic drag, eccentricity, and inclination damping on planetesimals. In addition to that, as described in Levison et al. (2012), LIPAD was built on top of SyMBA (Duncan et al. 1998) and developed so it has flags where one can turn on/off dynamical effects such as collisional evolution, dynamical friction, viscous stirring, planetesimal gravitational interactions, etc. Therefore, in its most basic form LIPAD behaves as SyMBA, but keeping its nature of being capable of tracking a large number of objects within tracer particles.

3. Capture Mechanism

We devote this section to reassessing the capture mechanism previously studied by Weidenschilling & Davis (1985), Malhotra (1993a), Beauge & Ferraz-Mello (1993), and Gomes (1995a, 1995b), and we highlight some of the main features that will be of major importance in our present work. In order to track the most basic dynamics and to better compare with the works above, all simulations in this section were conducted with LIPAD acting as SyMBA. In other words, no collisional evolution, dynamical friction, viscous stirring, or planetesimal gravitational interactions were considered.

As anticipated in the previous section, the works from Malhotra (1993a), Beauge & Ferraz-Mello (1993), and Gomes (1995a, 1995b) found that capture of small inward-drifting planetesimals subject to gas drag (see Rafikov 2005; Youdin 2010; Lambrechts & Johansen 2012, for a recent and complete description of all drag regimes) are more likely to occur when the small inward-drifting planetesimals approach the MMR with an eccentricity of the order of or larger than a specific value of equilibrium eccentricity (Equation (1)). Alternately, they can be captured if they drift slow enough in order to have their eccentricity pumped up to the equilibrium eccentricity during the MMR crossing. Figure 1 demonstrates this dynamic for the capture of an $r = 500$ m, $1.5 \times 10^{-9} M_{\oplus}$ tracer (representing $\sim 5.70 \times 10^{3}$ planetesimals with $2.63 \times 10^{-13} M_{\oplus}$ each) interacting with a $2 M_{\oplus}$ planet at 1 au. The importance of Figure 1 is not only to demonstrate the dynamics for the capture of planetesimals within MMRs but also to demonstrate that even a tracer particle representing many planetesimals in LIPAD will capture the dynamics of each planetesimal inside the tracer.

As can be seen in Figure 1, the swarm of $r = 500$ m planetesimals start their inward drift beyond the 2:1 MMR with the planet. Due to the gas damping effect acting on the eccentricity and inclination of the planetesimals, these values remain very low during the inward drift in between MMRs. On the other hand, every time the planetesimals cross an MMR, they strongly interact with the massive planet and receive a kick in their eccentricity that is proportional to the strength of that MMR (Beauge & Ferraz-Mello 1993; Malhotra 1993a). Whenever the kick in eccentricity is smaller than the equilibrium, or librational, eccentricity associated with that MMR, the planetesimals continue their inward drift and have their eccentricity damped again. This is the case of the 2:1, 3:2, and 4:3 MMR crossing. Only during the 5:4 MMR crossing do the eccentricities of the planetesimals grow to about the value of the librational eccentricity associated with the 5:4 MMR. Only then they are trapped. This is precisely the expected behavior that a single planetesimal would have (Beauge & Ferraz-Mello 1993; Malhotra 1993a), demonstrating that the dynamics of an inward-drifting swarm of planetesimals is well represented by the dynamics of our tracer particle.

The librational eccentricity can be estimated by the equation (Gomes 1995a, p. 55)[1]

$$e_{\rm lib} = 4\sqrt{\frac{k(1-\alpha)}{(16j+11k)\alpha}}, \quad (1)$$

where $(j + k)/j$ denotes the given MMR and α the ratio of the local circular velocity of the gas (v_g) over the Keplerian velocity (v_k) at the same heliocentric distance (d), so that $\alpha = v_g(d)/v_k(d)$. To determine α, we then need to know the local circular velocity of the gas. Similar to what can be found in Levison et al. (2010), using the description by Brasser et al. (2007), we can simply write

$$v_g(d) = v_k(d)\sqrt{1 - 2\eta(d)}, \quad (2)$$

where $\eta(d) = 4.55 c_s(d)/v_k(d)$, with the sound speed defined by $c_s(d) = 1.43 \times 10^3 (d/\text{au})^{(-1/4)}$ m s^{-1}.

A closer analysis of Equation (1) shows that $e_{\rm lib}$ for a given MMR increases as you go farther from the planet (see also Figures 4 and 11 in Beauge & Ferraz-Mello 1993; Malhotra 1993a, respectively), i.e., decreasing j in the $(j + 1)/j$ relationship. Also, as the MMR strength scales with the mass of the planet and α with heliocentric distance, it is expected that $e_{\rm lib}$ would be a function of the planet's distance from the star and of the size of the planetesimals. Therefore, it is expected that smaller planetesimals that drift faster will only be captured in very close-in MMRs where $e_{\rm lib}$ is small. Larger planetesimals, on the other hand, as they drift slower, can interact for longer times with MMRs and so acquire larger values of eccentricity, being captured in outer MMRs. Moreover, the closer the planet is to the star, the smallest size of a planetesimal that can be captured by a given MMR increases (Figure 2).[2]

Figure 2 shows the smallest radius of an inward-drifting planetesimal that can be captured in a given MMR. To build Figure 2, we considered 1000 tracers with radii ranging from $r = 0.01$ km to $r = 10$ km. As before, for each tracer we assumed $1.5 \times 10^{-9} M_{\oplus}$. This implies that the number of planetesimals inside the tracers will range from $\sim 7.12 \times 10^{8}$ planetesimals ($r = 0.01$ km) to $\sim 7.12 \times 10^{-1}$ planetesimals ($r = 10$ km). In terms of mass we have $\sim 2.1 \times 10^{-18} M_{\oplus}$ per planetesimal ($r = 0.01$ km) and $1.5 \times 10^{-9} M_{\oplus}$ for the single object represented by the $r = 10$ km tracer ($n_{\rm pl}$ smaller than unity). For this test all tracers were initially placed at the 3:2 MMR location and evolved until they were either captured or lost owing to collision with the planet, or by getting too close to the star. We performed three simulations, one for each position

[1] From long-term hydrodynamic simulations of planetesimals trapped in first-order MMRs Hsieh & Jiang (2019) found that the equilibrium eccentricity tends to be larger than predicted values in the literature. However, this is important for first-order resonances with $j < 5$ within the resonant relation $j/(j + 1)$, especially for the case of $j = 1$ (2:1 MMR in our notation). Therefore, as in our studied cases, most of the resonance trappings occur for values of $j \geqslant 7$; such underestimation of the values of $e_{\rm lib}$ should not be a problem. Indeed, the values predicted by Equation (1) seem to be a pretty good match according to Figure 1.

[2] An animation of the capture of different-sized planetesimals when considering a $2 M_{\oplus}$ planet at 1 au can be found electronically at http://www.boulder.swri.edu/~rdeienno/Capture.html.

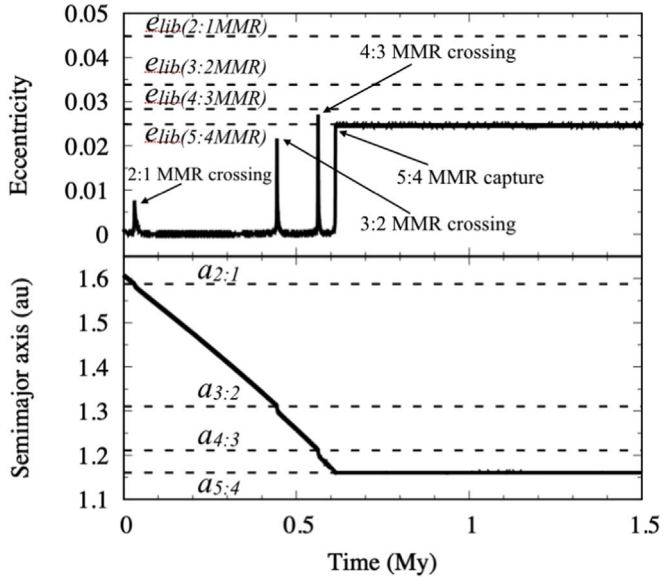

Figure 1. Capture of a swarm of $r = 500$ m planetesimals in the 5:4 MMR with a $2\,M_\oplus$ planet at 1 au. When crossing MMRs, the eccentricity of the planetesimals receives a kick proportional to the strength of the MMR and the time that they interact with the MMR. Only when the condition $e \geqslant e_{\rm lib}$ can capture happen. Top: evolution of the eccentricity. Bottom: evolution of the semimajor axis. The dashed lines in the top panel show, from top to bottom, the librational eccentricity ($e_{\rm lib}$) for the 2:1 MMR, 3:2 MMR, 4:3 MMR, and 5:4 MMR, respectively. The same in the bottom panel stands for the resonant semimajor axes $a_{2:1}$, $a_{3:2}$, $a_{4:3}$, and $a_{5:4}$, respectively.

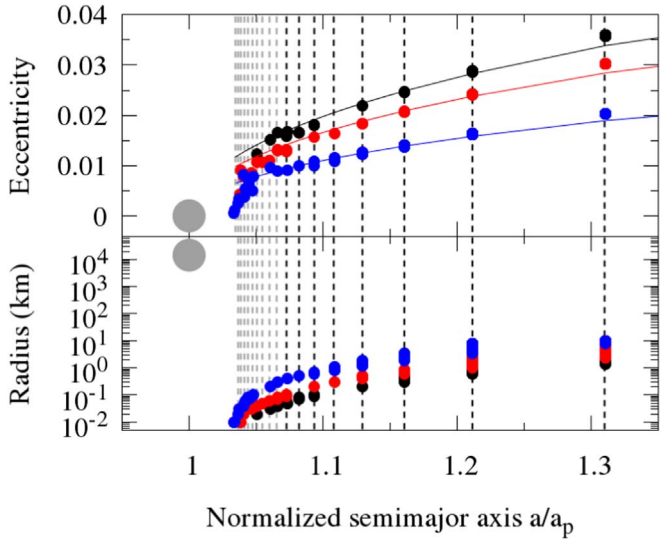

Figure 2. Size dependence and librational eccentricity for capture in MMR of small inward-drifting planetesimals in a gaseous environment as a function of the normalized semimajor axis (a/a_p). The large gray circle represents a $2\,M_\oplus$ planet. Small colored circles represent planetesimals of different sizes ($r = [0.01–10]$ km). The curved lines in the top panel represent the librational eccentricities calculated from Equation (1). The colors are, respectively, blue for the case where the planet is at 0.1 au, red at 0.5 au, and black at 1 au. The vertical dashed lines show all first-order MMRs from 20:10 to 11:10 (gray) and from 10:9 to 3:2 (black).

of the $2\,M_\oplus$ planet, at 0.1 au (blue), 0.5 au (red), and 1 au (black).

Although not shown, we performed several other simulations with different planet masses. The results were similar to what is shown in Figure 2. However, for a given semimajor axis, more massive planets capture smaller inward-drifting planetesimals and less massive planets capture larger inward-drifting planetesimals.

Finally, as we now know exactly how the capture works in our model and what size of inward-drifting planetesimal is more probable to be captured by a given MMR for a given planet's mass and distance from the star, in the following sections we will proceed with our study assuming different values of total mass for the tracers, as well as including planetesimal gravitational interaction and allowing for collisional evolution.

4. Dynamics with and without Collisional Evolution

The computational time required for our simulations is very large. Thus, we will consider a maximum of 10,000 tracers per simulation. Also, when collisional evolution is considered, the smallest tracer allowed in our simulations will have a radius $r_{\rm min} = 1$ m. To justify this, recall that many planetesimals can be represented by a single tracer, and that the planetesimals that compose the tracers do interact among themselves through statistical routines. Therefore, a larger number of massive tracers with small radii would represent a huge number of planetesimals, and with that comes an enormous increase in the demanded amount of statistical computation. Therefore, during collisional evolution, tracers that get smaller than $r_{\rm min}$ are removed from the simulation. This can also be justified by assuming that as planetesimals get more numerous and smaller in size, their collisional probability increases. Thus, it is reasonable to assume that they will collisionally grind to dust on short timescales. Also based on Figure 2, because small planetesimals experience fast inward drift, objects smaller than $r_{\rm min} = 1$ m (nearly the fastest drift rate) are very unlikely to get captured in any MMR.

Before we proceed to the next section, it is important to present the details of our calculations. Based on our experiments from Section 3, and to be as consistent as possible with the works from Levison et al. (2010), Batygin & Laughlin (2015), and Storch & Batygin (2019), knowing which size of inward-drifting planetesimal is more probable to be captured in each MMR, as a control setup, we will simulate the dynamics of a swarm of small $r = 100$ m inward-drifting planetesimals being captured by a $2\,M_\oplus$ planet at 1 au. Also, our simulations will be carried out in such a way that only one tracer per year will be added in the run. The location for tracer inclusion/addition will be set by the position of the resonant orbit at the beginning of the simulation (defined in Section 3). Once set, this location will be considered constant for the rest of the simulation. Thus, all simulations will start with only one single tracer, and only after 10,000 yr will all 10,000 tracers have been included in the runs. The reason for all this is simple: we want to minimize CPU time and test the scenario where capture would be near 100%.

As a final main note, it is important to say that, although we are concentrating our analyses in a swarm of $r = 100$ m inward-drifting planetesimals being captured by a $2\,M_\oplus$ planet at 1 au, by changing the total mass flux in planetesimals compared to the mass of the planet in the following sections, and considering the different sizes that the inward-drifting planetesimals can acquire during collisional evolution, we will be able to understand and predict what would happen for a wide range of possible scenarios.

4.1. Without Collisions

Before we start describing the experiments we made, it is important to have the following note and summary in mind. Due to the fact that we are proposing a pure numerical study, it is not within the scope of this work to provide any analytical treatment of the problem (we refer the reader to Storch & Batygin 2019 for a detailed and extensive analytical treatment of angular momentum transfer in the present scenario). Even so, for better understanding of the problem and discussion of the results presented, we summarize the main analytical findings by Storch & Batygin (2019), which quantified two situations for planet inward shepherding by resonant angular momentum transfer. First, Storch & Batygin (2019) showed that, in the case of a single inward-drifting planetesimal trapped in MMR, the rate of decay in semimajor axis of the planet is proportional to the ratio between the masses of the planetesimal and that of the planet (Storch & Batygin 2019, $\dot{a}_1/a_1 \propto m/m_1$, Equation (28), with the subscript 1 refering to the planet as denoted by the authors). Second, Storch & Batygin (2019) have quantified that the timescale for the planet's semimajor axis decay rate when considering a collection of massive inward-drifting planetesimals trapped in MMR (Storch & Batygin 2019, $1/t_{\rm ARM} \equiv -\dot{a}_1/a_1 \approx \chi^{3/2}(M_{\rm swarm}/m_1)$ in authors' notation, Equation (34), where $M_{\rm swarm}$ is the total mass of planetesimals trapped in MMR and χ of the order of 0.001–0.01). From the two situations considered by Storch & Batygin (2019) it becomes clear that a planet's inward shepherding by resonant angular momentum transfer is proportional to the total mass in MMR compared to that of the planet. Therefore, more mass within MMR means faster inward planet shepherding, and less mass means slower or negligible inward planet shepherding.

For our first simulations we will perform two cases, with and without planetesimal gravitational interactions but always with no collisional evolution. These should also be taken as control simulations, and we expect them to be the closest approach that our work will have to the findings presented in Levison et al. (2010) and Batygin & Laughlin (2015) (for the cases where planetesimals do not interact among themselves), as well as in Storch & Batygin (2019) (when gravitational interaction is considered). Four cases with different mass fluxes in inward-drifting planetesimals are considered, 0.1, 0.5, 2, and 20 $M_\oplus$. As collisional evolution is not taken into account, the radii of the tracers in each simulation will always be constant. Therefore, in each simulation the constant numbers of $r = 100$ m massive inward-drifting planetesimals represented by each tracer are $\sim 4.75 \times 10^9$, $\sim 2.37 \times 10^{10}$, $\sim 9.50 \times 10^{10}$, and $\sim 9.50 \times 10^{11}$, respectively. The tracer inclusion will follow the description given in Section 4, with the resonant location defined as the 8:7 MMR.

Figure 3 shows the results of the simulations and Table 1 a summary of the results. As can be seen from Figure 3, in all cases, the 2 $M_\oplus$ planet is easily pushed inward by the massive swarm of small inward-drifting planetesimals. One can also notice that larger fluxes of inward-drifting planetesimals push the planet more efficiently. For example, from Figure 3, bottom right, we observe that only a few tracers are needed to be in MMR in order to start shepherding the planet owing to resonant angular momentum transfer. The opposite occurs in the top left panel of Figure 3, where only after all 10,000 tracers and therefore the total 0.1 $M_\oplus$ in planetesimals get captured in MMR do the planet starts moving. This is expected if we consider that in the former case only 50 tracers will already represent 0.1 $M_\oplus$, and that, as discussed in the first paragraph of this section, planet shepherding is proportional to the total mass of inward-drifting planetesimals trapped in MMR compared to the mass of the planet.

It is remarkable that when gravitational interaction is considered among the planetesimals, no visual changes are observed when comparing the results with the cases where planetesimals do not gravitationally interact (Storch & Batygin 2019). This can be interpreted by the fact that, although tracers can be very massive, the small planetesimals that compose the tracers each carry small mass (proportional to their sizes). The only visual change between simulations with and without planetesimal gravitational interaction appears for the 20 $M_\oplus$ flux case (Figure 3, bottom right). Still, the global evolution and the final result are not very different from each other.

As previously said in Section 4, by including tracers/planetesimals over time at the location of the MMR, we attempt to maximize capture efficiency. In the case of Figure 3, top left, tracers are very low in mass (compared to the mass of the planet). Thus, they are only able to start shepherding the planet inward after all of them are captured in a single MMR. Therefore, in this case, all tracers/planetesimals do get captured and follow the predicted MMR from Section 3. In the other cases, the planet usually starts being shepherded inward prior to all tracers being included in the simulation. This results in the following. As the planet moves inward, it reaches denser portions within the gas disk. The same happens to the planetesimals already captured in the MMR predicted from the experiments and theory in Section 3. In a denser environment planetesimals drift faster. Thus, as the planet gets closer to the star, the faster the planetesimals that are shepherding the planet inward will drift (transferring more angular momentum). Still, small planetesimals tend to continue drifting faster than the overall drift of the planet being shepherded inward. Thus, even the late included tracers can reach and cross the planet's MMRs. Moreover, these late included tracers now move relatively slower with respect to the moving planet. This happens as a result of the difference in the relative drifting velocity of the planet (zero in the beginning and nonzero afterward) to that of the late included planetesimals (both in the same direction). The resultant longer time interaction planetesimals/MMRs cause the inward-drifting planetesimals to reach $e_{\rm lib}$ for outer MMRs (not possible when the planet is not drifting). That is the reason why we see inward-drifting planetesimals captured in slightly farther MMRs in the top right and bottom left panels of Figure 3. In the most extreme case, where tracers are very massive (Figure 3, bottom right), we do not need many tracers to start pushing the planet toward the star. Thus, the planet starts moving very soon in the simulations. Moreover, it reaches denser portions of the gas disk faster, and its inward-drifting velocity can become so high that some late included planetesimals can either decouple from more distant outer MMRs or never catch up with the planet's close-in MMRs. That is the reason why we see planetesimals drifting slower than the planet in these panels after about 10,000–20,000 yr.

We can finish saying that these control simulations do confirm the findings presented by Levison et al. (2010), Batygin & Laughlin (2015) and Storch & Batygin (2019), no

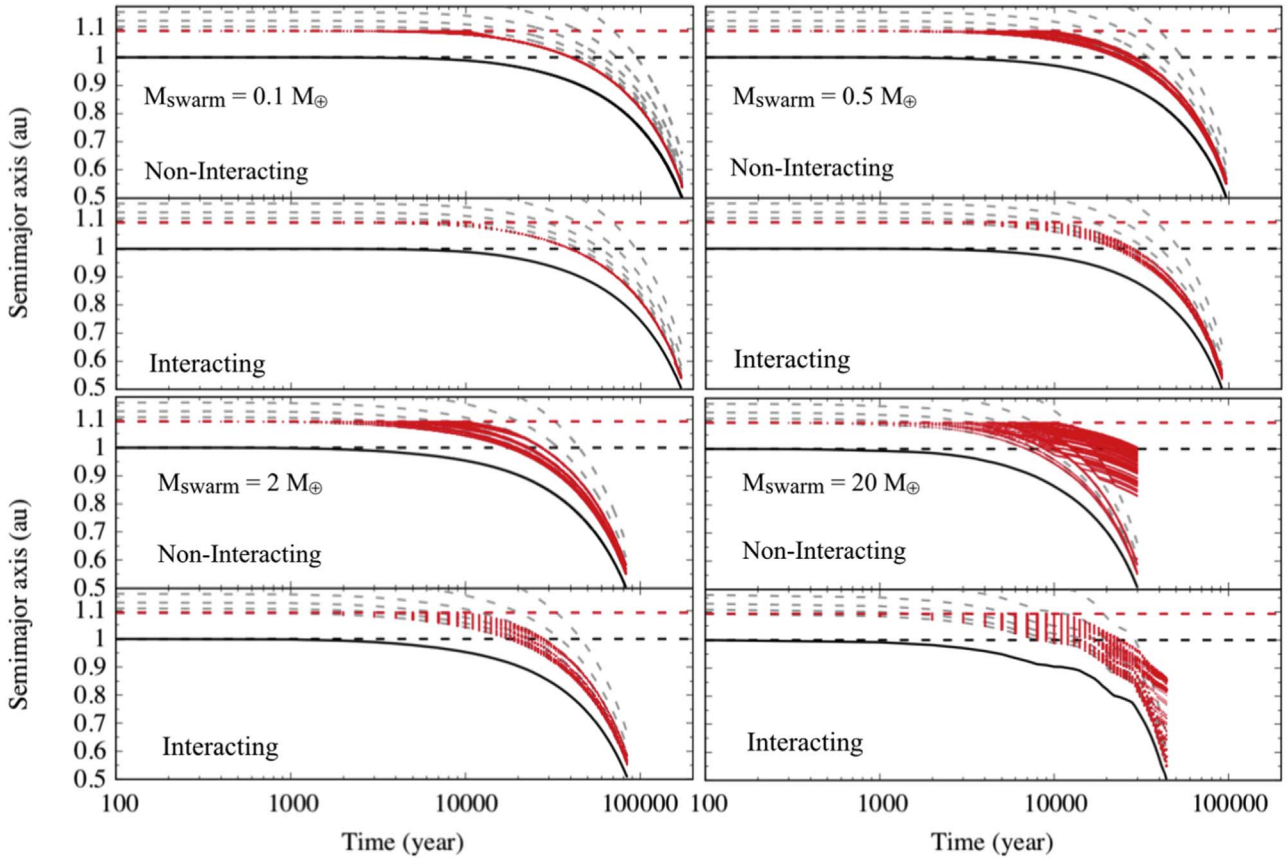

Figure 3. Semimajor axis as a function of time for a 2 $M_\oplus$ planet being shepherded inward by a large flux of $r = 100$ m massive inward-drifting planetesimals captured in MMRs. Solid black line: semimajor axis of the planet. Dotted red lines: semimajor axes of the planetesimals. Total mass in $r = 100$ m planetesimals—Top left: 0.1 $M_\oplus$ (1 tracer ~4.75×10^9 planetesimals). Top right: 0.5 $M_\oplus$ (1 tracer ~2.37×10^{10} planetesimals). Bottom left: 2 $M_\oplus$ (1 tracer ~9.50×10^{10} planetesimals). Bottom right: 20 $M_\oplus$ (1 tracer ~9.50×10^{11} planetesimals; Batygin & Laughlin 2015). The mass $m_{\rm pl}$ of a single planetesimal inside a single tracer particle is about 2.10×10^{-15} $M_\oplus$ in all cases. The dashed horizontal lines are (for reference) the initial semimajor axis of the planet (black) and the original location of the MMR (8:7 when the planet is at 1 au for $r = 100$ m planetesimal) that the tracers will be injected over time in simulation (red). The gray dashed lines represent the path of the MMRs when the planet's semimajor axis is evolving. The MMRs shown are all first order from 8:7 to 3:2. The labels "Noninteracting" and "Interacting" refer to the cases with and without planetesimal gravitational interaction, respectively. The total mass in the inward-drifting planetesimal swarm is also presented in the top panel of each case.

Table 1
Summary of Results from Figure 3

$M_{\rm swarm}$ ($M_\oplus$)	Gravitational Interaction	Collisional Evolution	Inward Shepherding
0.1	×	×	✓
0.1	✓	×	✓
0.5	×	×	✓
0.5	✓	×	✓
2	×	×	✓
2	✓	×	✓
20	×	×	✓
20	✓	×	✓

Note. $M_{\rm planet} = 2\,M_\oplus$ in all cases.

matter whether gravitational interaction among planetesimals is considered or not.

4.2. With Collisions

Now we introduce collisional evolution as described in Sections 2 and 4, i.e., the statistical routines in LIPAD will check for collisions among all the planetesimals inside all the tracer particles, and then apply the theory described in Benz & Asphaug (1999, by assuming Q_d^* (the kinetic energy per unit of mass of the target) for basaltic planetesimals with the coefficients associated to $v_{\rm impact} = 5$ km s^{-1} in their Table 3) to determine the new radii for the largest remnant and possible fragments of planetesimals resulting out of such events.

4.2.1. An Instructive Case

Instead of simply rerunning the simulations from the last section with collisional evolution, we first explore an instructive case with less total mass in inward-drifting planetesimals but larger planetesimal size ($r = 1$ km). This instructive case provides for a slower evolution of the massive inward planetesimal swarm, easing vizualization of the key dynamics that change with the inclusion of collisional evolution. We then return to our primary test cases.

The setup for our instructive experiment considers, as before, a 2 $M_\oplus$ planet at 1 au, but now a total mass flux in inward-drifting planetesimals equal to $\sim 10^{-3}$ $M_\oplus$ (about 2 times the current mass in the main asteroid belt; DeMeo & Carry 2013). Again the tracer inclusion will follow the description given in Section 4, but now with the resonant location defined as the 4:3

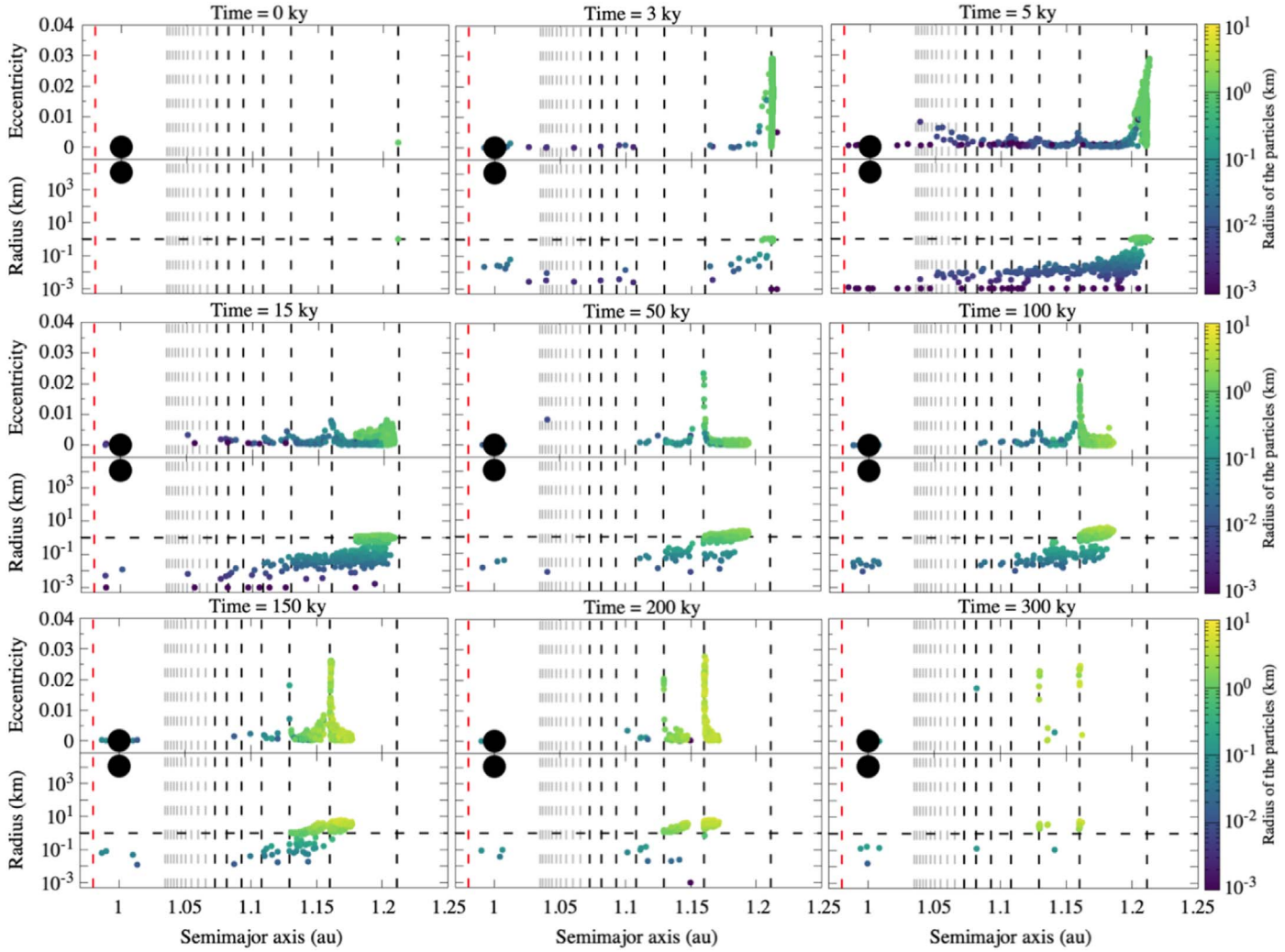

Figure 4. Snapshots of the collisional evolution of a swarm of massive inward-drifting planetesimals (small colored circles) with initial size $r = 1$ km injected in the 4:3 MMR (rightmost vertical dashed line) with a 2 $M_\oplus$ planet (large black circle). The total mass in 10,000 tracers, representing a total of $\sim 475 \times 10^6$ ($r = 1$ km) planetesimals ($\sim$47,500 planetesimals per tracer; $m_{\rm pl} \sim 2.10 \times 10^{-12}\, M_\oplus$), is 2 times the main asteroid belt mass ($\sim 10^{-3}\, M_\oplus$; DeMeo & Carry 2013). The vertical dashed lines show all first-order MMRs from 20:10 to 11:10 (gray) and from 10:9 to 4:3 (black), as well as the distance from the Sun from where planetesimals are eliminated from the simulation ($a = 0.98$ au; red). The horizontal dashed line in black (bottom panels) indicates 1 km for reference.

MMR. Figure 4 shows snapshots of the evolution of the massive swarm of $r = 1$ km inward-drifting planetesimals.[3]

As expected from the experiments in the previous section (see first paragraph of Section 4.1.), the total mass considered in this experiment (two orders of magnitude smaller than that from Figure 3, top left) is not sufficient to push a 2 $M_\oplus$ planet (also pointed out by Batygin & Laughlin 2015).

Still, as can be remarkably seen in Figure 4, even such a small amount of total mass (small when compared to the mass of the planet) already provides substantial collisional evolution. The evolution presented in Figure 4 and the linked animation shows that (i) the planetesimals injected in the 4:3 MMR evolve to the equilibrium eccentricity associated, and (ii) once enough mass accumulates in the MMR, with nonzero eccentricity, the massive planetesimals either escape the resonance, due to viscous stirring, or collisionally evolve. In the first case, the planetesimals keep their size ($r = 1$ km) unchanged and drift inward toward the next interior MMR. There, they will be captured again, as predicted by the theory in Section 3. For the planetesimals that remain captured in the MMR and instead collisionally evolve, they very likely break into smaller pieces. This can be seen in Figure 4, where small-radius particles start to be produced. These smaller generated fragments, no longer able to be captured by the local MMR (Section 3), can drift inward a lot faster, bypassing most of the interior MMRs and even the planet (or getting accreted by the planet). Those that eventually get captured in some inner MMR pile up with others, and processes (i) and (ii) repeat until almost no planetesimal survives.

As a final note, it is important to attend to the fact that, as the broken fragments are very small ($r \lesssim 100$ m), they migrate inward so fast that their direct interaction with the planet is negligible. In other words, the planet does not have enough time to interact with these inward-drifting particles, nor does it scatter these particles (particle eccentricities are always near zero close to the planet's location). Also, especially in the case considered in this section, the total mass over time that bypasses the planet's orbit is too small compared to the planet's mass in order to cause any effect, e.g., planetesimal driven

[3] An animation of the entire evolution can be found at http://www.boulder.swri.edu/~rdeienno/ColEvo.html.

migration (PDM; Fernandez & Ip 1984; Levison et al. 2010; Minton & Levison 2014; see discussion in the next section).

4.2.2. More Massive Planetesimal Fluxes

In these following Sections 4.2.2 and 4.2.3, different from the instructive case considered in the previous Section 4.2.1, the total mass within inward-drifting small fragments of planetesimals can be of the order of the planet's mass or higher. The direct gravitational interaction between inward-drifting small fragments of planetesimals and the planet might not be negligible. The main outcome of this interaction is PDM (Fernandez & Ip 1984; Malhotra 1993b; Ida et al. 2000; Levison et al. 2010; Nesvorný & Morbidelli 2012; Minton & Levison 2014; Deienno et al. 2017; Quarles & Kaib 2019). Ida et al. (2000) found that PDM should be self-sustained once the timescale for scattering planetesimals from the planet's feeding zone was longer than the migration timescale of the planet. Minton & Levison (2014) also reported that the migration rate of a planet due to PDM is set by the amount of mass available for it to scatter. Therefore, PDM only happens if the planet gravitationally scatters an appreciable fraction of its mass. This is different physics than resonant angular momentum transfer due to planetesimals trapped in MMRs as discussed in Section 4.1. It is also worth noting that some planetesimals can drift so fast (the smallest ones—typically fragments of collisional evolution) that they are effectively not scattered at all by the planet and contribute no angular momentum to its orbit. Once again, we stress that, although it is beyond the scope of this work to provide extensive analytical formulations (we refer the reader to Ida et al. 2000 and Minton & Levison 2014, for a detailed description and analytical treatment about PDM), we provide the reader with a summary of important metrics to better understand our results and discussions.

Following Minton & Levison (2014, and references therein), we find that the migration rate due to PDM is proportional to the ratio between the collective mass of planetesimals being scattered by the planet at a given time and the planet's mass ($|da/dt| \propto M_{\rm enc}/M_p$; Minton & Levison 2014, Equation (4), with $M_{\rm enc}$ the total instantaneous mass in planetesimals that encounters the planet, and M_p the mass of the planet, as in the authors' notation). Translating this formulation into our scenario implies that, unless there is a continuous stream of non negligible amount of mass in inward-drifting planetesimals encountering the planet's Hill sphere for a long enough time, PDM should not be self-sustained, or not observed at all.

With the above in mind, in this section we reassess the exact simulations from Section 4.1 (those where we have considered gravitational interaction among planetesimals), and we include collisional evolution for planetesimals as described in Sections 4.2 and 4.2.1.

Similarly to Figures 3 and 4, Figure 5 shows snapshots of the collisional evolution of the massive swarm of small inward-drifting planetesimals and the temporal evolution of the semimajor axes of the planetesimals and planet. Table 2 shows a summary of the results. As expected from previous results shown in Section 4.2.1 and Figure 4, by increasing the mass inside the MMR, we also increase the collisional rate, and therefore more grinding is observed. Both the grinding and the fast inward drifting of the small generated fragments can be seen in all of the panels from Figure 5.

What needs to be pointed out when comparing Figures 3 and 5 is that when collisional evolution is considered, even a very large flux of $r = 100$ m massive inward-drifting planetesimals is not able to push the $2\,M_\oplus$ planet inward. As can be seen in panels (A)–(C) of Figure 5, the global evolution is very similar to, although much faster than, what was observed in Figure 4. That is, as soon as enough mass accumulates within a given MMR, the massive planetesimals either leave the MMR, due to viscous stirring, or collisionally evolve. In the latter case, they usually bypass or accrete into the planet. Therefore, as one can see from panels (A)–(C) in Figure 5, in no case are significant changes appreciated in the planet's semimajor axis. This can be interpreted as a result of two factors. First, as the planetesimals within MMRs rapidly collisionally evolve and leave the MMRs, they do not represent enough mass trapped in MMR in order to transfer angular momentum via resonant lock to the planet (see discussion in the first paragraph of Section 4.1). Therefore, there is no inward shepherding of the planet. Second, in the case for panels (A)–(C) from Figure 5, there is not enough continuous mass in inward-drifting planetesimals hitting the planet's Hill sphere in order to provide for outward PDM (see discussion in the first paragraph of this section).

Additionally, two striking dynamical evolutions visible in Figure 5 have to be discussed:

1. The capture of small inward-drifting fragments of planetesimals in 1:1 MMR with the planet, as also noticed in the bottom panels of Figure 4 and associated animation. Although not studied in detail in the present work, those captures are real and predicted. Recall from Section 3 that capture becomes probable when $e \geqslant e_{\rm lib}$ and that $e_{\rm lib}$ decreases for distances closer to the planet (Equation (1), and Figures 1 and 2). In the case of the 1:1 MMR ($k = 0$ in the $(j + k)/j$ relationship), $e_{\rm lib}$ equals zero (Equation (1)). Therefore, although still not 100% probable (Beauge & Ferraz-Mello 1993; Malhotra 1993a; Gomes 1995a, 1995b), 1:1 MMR trojan capture should be expected at some level. Moreover, as collisions in this regime occur at nearly zero eccentricity orbits, growth is much more likely owing to low-velocity collisions, leading to the formation of a few $r \sim 10$ km objects within 100,000 yr. However, as previously said, we did not study in detail either the capture or the subsequent collisional evolution/stability of such trojan objects. This is by itself a very interesting subject. We leave that for future work.
2. Figure 5(D) shows outward PDM for the planet ($\Delta a \approx 0.07$ au). As previously discussed, collisions are more likely to break planetesimals into very small fragments. These small generated fragments often drift across the orbit of the planet without being captured. A very large flux of $20\,M_\oplus$, as considered in the experiment of Figure 5(D) (similar to that from Batygin & Laughlin 2015), rather causes the planet to migrate outward instead of being pushed inward (see also Figure 4 in Levison et al. 2010). This is because, as previously discussed in the beginning of this section, when planetesimals are crossing the orbit of the planet (coming from far out), by interacting with the planet, they may get scattered inward (if not drifting too fast). Therefore, as a consequence of the conservation of angular momentum, the planet has to move outward. Furthermore, differently than in the cases of panels (A)–(C) from Figure 5, here a

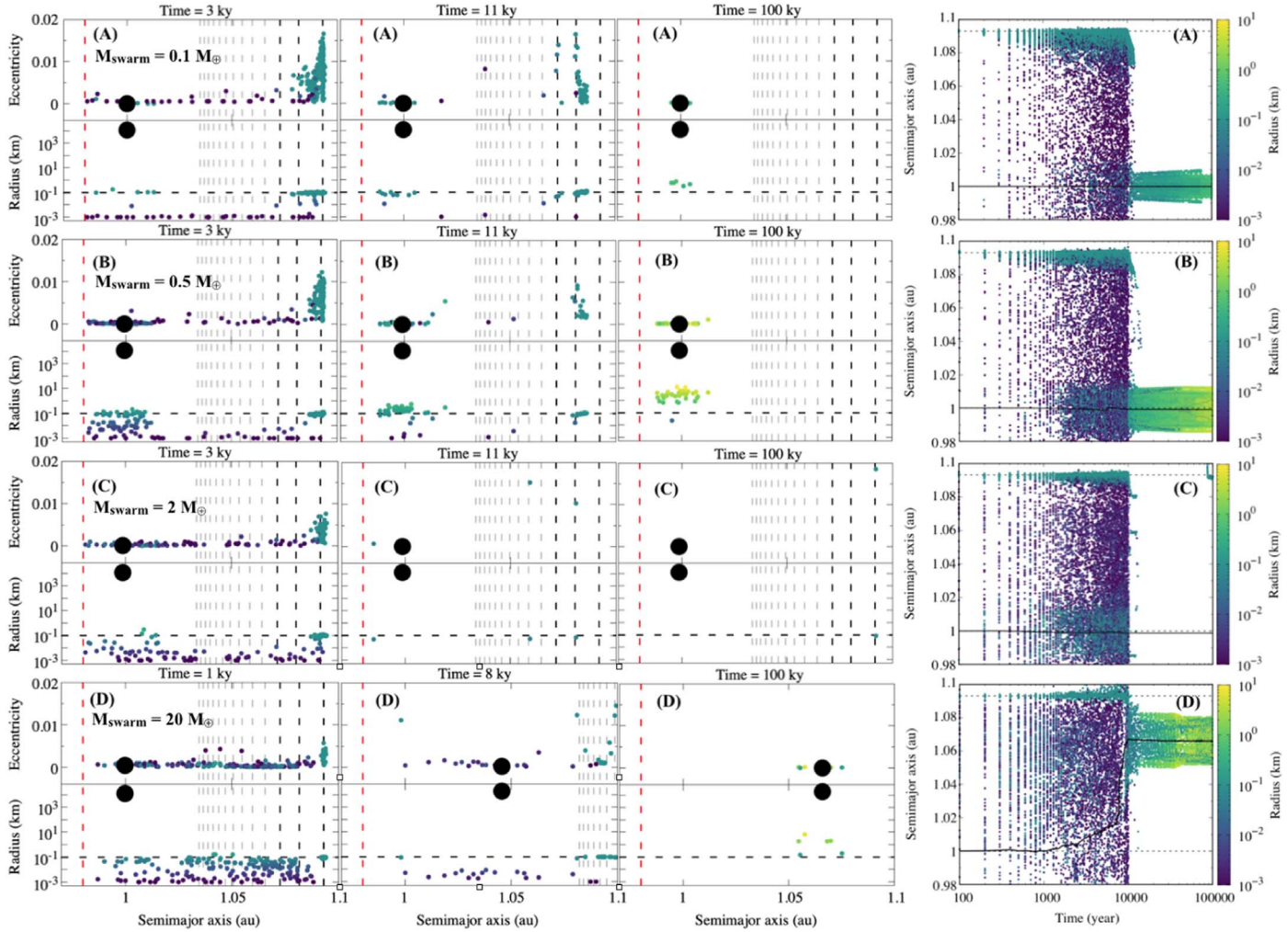

Figure 5. First three column panels (A)–(D) from left to right: snapshots of the collisional evolution of a swarm of massive inward-drifting planetesimals (small colored circles) with initial size $r = 100$ m injected in the 8:7 MMR (rightmost vertical dashed line) with a 2 $M_\oplus$ planet (large black circle). Total mass in $r = 100$ m planetesimals—(A) 0.1 $M_\oplus$ (1 tracer $\sim 4.75 \times 10^9$ planetesimals). (B) 0.5 $M_\oplus$ (1 tracer $\sim 2.37 \times 10^{10}$ planetesimals). (C) 2 $M_\oplus$ (1 tracer $\sim 9.50 \times 10^{10}$ planetesimals). (D) 20 $M_\oplus$ (1 tracer $\sim 9.50 \times 10^{11}$ planetesimals; Batygin & Laughlin 2015). The mass $m_{\rm pl}$ of a single planetesimal inside a single tracer particle is about 2.10×10^{-15} $M_\oplus$ in all cases. The vertical dashed lines show all first-order MMRs from 20:10 to 11:10 (gray) and from 10:9 to 8:7 (black), as well as the distance from the Sun from where planetesimals are eliminated from the simulation ($a = 0.98$ au; red). The horizontal dashed line in black (bottom panels) indicates 100 m for reference. The rightmost panels in (A)–(D) show the entire evolution of the semimajor axis of the planet (solid black line) and of the collisionally evolved planetesimals, with their radius represented by the color bar. The dashed horizontal lines in these rightmost panels are the initial semimajor axis of the planet (black) and the original location of the MMR (8:7 when the planet is at 1 au for $r = 100$ m planetesimal) that the tracers will be injected over time in simulation (gray). The total mass in the inward-drifting planetesimal swarm is also presented in the leftmost top panel of each case.

Table 2
Summary of Results from Figure 5

$M_{\rm swarm}$ ($M_\oplus$)	Gravitational Interaction	Collisional Evolution	Inward Shepherding	Outward PDM
0.1	✓	✓	×	×
0.5	✓	✓	×	×
2	✓	✓	×	×
20	✓	✓	×	✓[a]

Notes. $M_{\rm planet} = 2\ M_\oplus$ in all cases. Q_d^* (Benz & Asphaug 1999) for collisions.
[a] $\Delta a_{\rm planet} \approx 0.07$ au.

total of 20 $M_\oplus$ does provide enough continuous stream of mass in inward-drifting planetesimals' fragments hitting the planet's feeding zone in order to provide for outward PDM (Minton & Levison 2014). Even so, the amount of PDM provided is very small ($\Delta a \approx 0.07$ au) compared to the total mass bypassing the orbit of the planet (20 $M_\oplus$). This is because only a small portion of the mass in planetesimals drifting inward gets scattered by the planet. The majority of the inward-drifting planetesimals, often in very small sizes ($r \approx 1$–10 m), drift so fast that they do not interact with the planet long enough to be scattered.

With that said, by putting the findings from all previous sections together, we can infer what effects changing planetesimal sizes and planets' mass and distance from the star would cause in the main results, especially related to the possibility of planet inward shepherding due to angular momentum transfer by inward-drifting planetesimals trapped in MMRs (the goal of this study).

Changing planetesimal sizes would most likely have no major influence because larger planetesimals drift a lot slower and therefore do not have enough momentum to transfer to the orbit of the planet via resonant lock. These larger planetesimals

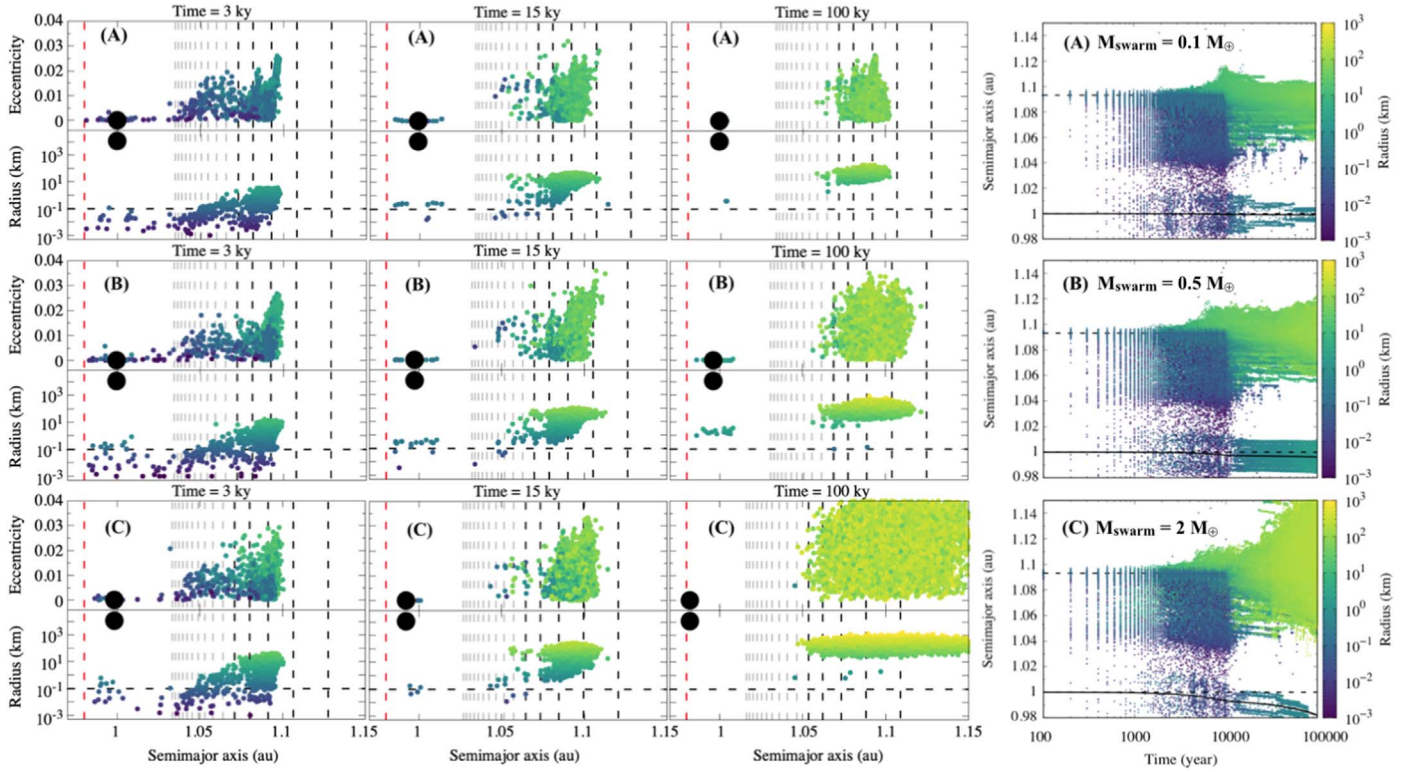

Figure 6. Same as in Figure 5, but now considering $Q^*_{d100} = 100Q^*_d$ (Benz & Asphaug 1999). (A) Total mass in $r = 100$ m planetesimals equal to 0.1 $M_\oplus$ (1 tracer $\sim 4.75 \times 10^9$ planetesimals). (B) 0.5 $M_\oplus$ (1 tracer $\sim 2.37 \times 10^{10}$ planetesimals). (C) 2 $M_\oplus$ (1 tracer $\sim 9.50 \times 10^{10}$ planetesimals). The mass $m_{\rm pl}$ of a single planetesimal inside a single tracer particle is about 2.10×10^{-15} $M_\oplus$ in all cases. The total mass in the inward-drifting planetesimal swarm is also presented in the rightmost panel of each case.

Table 3
Summary of Results from Figure 6

$M_{\rm swarm}$ ($M_\oplus$)	Gravitational Interaction	Collisional Evolution	Inward Shepherding
0.1	✓	✓	×
0.5	✓	✓	×
2	✓	✓	✓[a]

Notes. $M_{\rm planet} = 2\ M_\oplus$ in all cases. $Q^*_{d100} = 100Q^*_d$ for collisions.
[a] $\Delta a_{\rm planet} < 0.02$ au.

could get captured in farther MMRs (Figure 2), but as they do not transfer momentum fast enough, we can predict that they would rather accumulate in MMR and then evolve as in Figure 4 (case for $r = 1$ km planetesimals), breaking into smaller fragments that would eventually get captured in closer MMRs, thus evolving as shown in Figure 5 (case for $r = 100$ m planetesimals). Smaller planetesimals, on the other hand, would just not get captured (e.g., case for $r \sim 1$–10 m planetesimals in Figure 5). Meanwhile, changing the distance of the planet from the star would cause smaller planetesimals to be captured by a given MMR if the planet is moved away from the star and larger planetesimals to be captured in the same MMR if the planet is closer to the star (Figure 2).

Changing the mass of the planet, on the other hand, would change the amount of momentum needed to be transferred via resonant lock in order to cause changes in the planets's orbit. A more massive planet would demand even more massive fluxes than those considered in this work. Even if possible to be accessed, more massive fluxes would imply more grinding (Bottke et al. 2005), and the result would still be somewhere among the cases shown in Figure 5. Less massive planets would need less momentum to be transferred via resonant lock. However, as discussed in Section 3, the capture probability is related to the strength of the MMR (proportional to the mass of the planet) and to the amount of time that the inward-drifting planetesimal interacts with the MMR (its size). This means that less massive planets would necessarily capture larger (slower inward-drifting) planetesimals per MMR. Therefore, we conclude that the dynamics would not be different than what we presented in Figure 4, and that it would scale in mass with what we presented in Figure 5.

Finally, one thing that still needs to be tested is the influence of the material strength of such small planetesimals. For that, we dedicate the following section.

4.2.3. The Implications of Q^*_d

Until this point, we have only considered planetesimals with Q^*_d as described in Benz & Asphaug (1999; see Section 4.2 above). However, it is not clear what would be the strength of the materials that compose small planetesimals, mainly because we do not know the real composition of planetesimals. More fragile planetesimals (with smaller values for Q^*_d) would break more easily than we observed previously. Thus, those would certainly not cause any changes to the results obtained. Therefore, we expect that only planetesimals with more material strength could cause differences in the collisional evolution and overall results.

With that said, in this section we rerun the simulations of Section 4.2.2 but now considering an increase in the Q^*_d. We carried out simulations with $Q^*_{d10} = 10Q^*_d$, $Q^*_{d100} = 100Q^*_d$,

and $Q^*_{d1000} = 1000Q^*_d$. Given the similarity in the results among simulations with the increased Q^*_d values, we will focus our discussion on only one of them. We chose the intermediate value, $Q^*_{d100} = 100Q^*_d$ (Figure 6).

Figure 6 shows the results for such simulations, and a summary of the results is given in Table 3. As can be seen, when planetesimals are made harder to break, they grow during collisions. The growth of such planetesimals slows down their inward-drifting velocity. Therefore, because the planetesimals keep growing by constructive collisions and drifting more and more slowly as they grow, once again not enough momentum can be transferred via resonant interaction to the orbit of the planet. The only measurable change in the planet's semimajor axis is observed in Figure 6(C), where a $2\,M_\oplus$ flux of $r = 100$ m inward-drifting planetesimals was considered. However, it is also noticed in this figure that the growth of planetesimals takes over and many $r \gtrsim 500$ km are formed within 100 kyr. This also explains the spreading of objects near the MMR location, which is associated with a very large stirring from large objects forming close to each other. Although not expected at first, this is not entirely surprising if we consider that $2\,M_\oplus$ is the total mass in planetesimals considered by Walsh & Levison (2016) and Deienno et al. (2019) within 0.7 au and 1 au to build up the whole terrestrial planet system observed in our solar system. Still, although measurable, the change in semimajor axis observed in Figure 6(C) is almost negligible when compared to our control simulation shown in the bottom left panel of Figure 3 ($\Delta a < 0.02$ au compared to $\Delta a \geqslant 0.5$ au).

Due to computational time restrictions, we were not able to perform in this section a simulation with the total flux of $20\,M_\oplus$ in $r = 100$ m inward-drifting planetesimals. Still, as before, we can extrapolate the expected results based on what was presented in the previous experiments. The expected conclusion is that, given that a flux of $2\,M_\oplus$ already started forming planetary cores around the MMR location where planetesimals were captured, even if a $20\,M_\oplus$ flux of inward-drifting planetesimals would be able to shepherd inward the $2\,M_\oplus$ planet over larger distances, other new large planets would very likely form near the MMR location, possibly substituting the old planet.

The experiments in this section are good at validating the overall conclusion that planet inward shepherding by a large swarm of small massive inward-drifting planetesimals is very unlikely.

5. Conclusion

It was reported in the works by Levison et al. (2010, see Figure 6 in their paper), Batygin & Laughlin (2015), and Storch & Batygin (2019) that a massive swarm of fast inward-drifting small (meter- to kilometer-sized) planetesimals caught in MMR with planets would possibly shepherd the planets inward by means of angular momentum transfer via resonant lock. Although appealing, it was not clear whether or not such an inward shepherding feature would hold when collisional evolution is considered. This is because, as anticipated by Weidenschilling & Davis (1985) and briefly discussed in Levison et al. (2010), inward-drifting planetesimals trapped in resonance with planets have their eccentricity increased by the interaction with the planet. As a result, the orbit of these planetesimals can eventually cross others and potentially increase the chance and speed for collisions. Therefore, the main purpose of this work became the investigation of how this massive swarm of small inward-drifting planetesimals would interact and collisionally evolve when captured in MMR with a planet.

To perform this task, we first reassessed the MMR capture mechanism of small inward-drifting planetesimals by planets when subjected to gas drag effects. We showed which sizes of inward-drifting planetesimals are more likely to be captured by a given external MMR as a function of the planet's mass and distance from the star (Section 3). In agreement with Malhotra (1993a), Beauge & Ferraz-Mello (1993), and Gomes (1995a, 1995b), we showed that capture can only occur for inward-drifting planetesimals that reach a given MMR with eccentricity similar to or larger than an equilibrium (librational) eccentricity value associated with that MMR. In addition, we showed how the equilibrium eccentricity varies with distance. Therefore, we concluded that small inward-drifting planetesimals (meter sized) are more likely to be captured by very massive planets or when the planet is far from the host star. For planets close to a star or with small mass, only large inward-drifting planetesimals (kilometer sized) can be captured by exterior MMRs.

In Section 4.1 we demonstrated the findings from Levison et al. (2010), Batygin & Laughlin (2015), and Storch & Batygin (2019) by considering four cases where a massive swarm of inward fast drifting planetesimals push a $2\,M_\oplus$ planet inward by 0.5 au within 100 kyr. This was demonstrated for both cases where planetesimals interact and do not interact among themselves. Then, in the following Sections 4.2.1–4.2.3 we included collisional evolution to the same simulations from Section 4.1. We also considered different sizes and material strength for the planetesimals, as well as discussed the influences that the mass and location of the planet would have in our results. The conclusion was very straightforward. Small massive inward-drifting planetesimals in MMR rapidly collisionally evolve. Depending on the scaling law (Benz & Asphaug 1999; Q^*_d) assumed, there are two main consequences. One is that the inward-drifting planetesimals decrease in size owing to collisional breakup and leave the MMR (particle–gas interactions result in planetesimal drifting rate being proportional to the inverse of the planetesimal size). The other is that they grow during collisional events, thus slowing down or even stopping their inward drift (depending on how much they grow).

In summary, no significant changes were observed in the planet's semimajor axis due to inward shepherding when collisional evolution is considered (independently of mass and size of the planetesimals). Therefore, we conclude that collisional evolution prevents planet inward shepherding aided by a massive swarm of small (meter- to kilometer-sized) inward-drifting planetesimals.

Furthermore, we would like to point out that, although the present work was motivated by the solar system's problems (Levison et al. 2010; Batygin & Laughlin 2015), the results presented are entirely valid for any planetary system.

We acknowledge an anonymous reviewer for very constructive comments that provided a substantial improvement of this work. R.D., K.J.W., H.L., and K.K. were supported by NASA's ATP, EW, and SSERVI programs.

ORCID iDs

Rogerio Deienno https://orcid.org/0000-0001-6730-7857
Kevin J. Walsh https://orcid.org/0000-0002-0906-1761
Katherine A. Kretke https://orcid.org/0000-0001-9601-878X

References

Adachi, I., Hayashi, C., & Nakazawa, K. 1976, PThPh, 56, 1756
Batygin, K., & Laughlin, G. 2015, PNAS, 112, 4214
Beauge, C., & Ferraz-Mello, S. 1993, Icar, 103, 301
Benz, W., & Asphaug, E. 1999, Icar, 142, 5
Bottke, W. F., Durda, D. D., Nesvorný, D., et al. 2005, Icar, 175, 111
Brasser, R., Duncan, M. J., & Levison, H. F. 2007, Icar, 191, 413
Chrenko, O., & Broz, M. 2015, AAS/DPS Meeting, 47, 418.02
Deienno, R., Morbidelli, A., Gomes, R. S., & Nesvorný, D. 2017, AJ, 153, 153
Deienno, R., Walsh, K. J., Kretke, K. A., et al. 2019, ApJ, 876, 103
DeMeo, F. E., & Carry, B. 2013, Icar, 226, 723
Duncan, M. J., Levison, H. F., & Lee, M. H. 1998, AJ, 116, 2067
Fernandez, J. A., & Ip, W.-H. 1984, Icar, 58, 109
Gomes, R. S. 1995a, Icar, 115, 47
Gomes, R. S. 1995b, CeMDA, 61, 97
Hayashi, C. 1981, PThPS, 70, 35
Hayashi, C., Nakazawa, K., & Nakagawa, Y. 1985, in Protostars and Planets II, ed. D. C. Black & M. S. Matthews (Tucson, AZ: Univ. Arizona Press), 1100
Hsieh, H.-F., & Jiang, I.-G. 2019, ApJ, 877, 34
Ida, S., Bryden, G., Lin, D. N. C., et al. 2000, ApJ, 534, 428
Jiang, I.-G., & Yeh, L.-C. 2004, MNRAS, 355, L29
Lambrechts, M., & Johansen, A. 2012, A&A, 544, A32
Levison, H. F., & Duncan, M. J. 2000, AJ, 120, 2117
Levison, H. F., Duncan, M. J., & Thommes, E. 2012, AJ, 144, 119
Levison, H. F., Thommes, E., & Duncan, M. J. 2010, AJ, 139, 1297
Lissauer, J. J., Fabrycky, D. C., Ford, E. B., et al. 2011, Natur, 470, 53
Malhotra, R. 1993a, Icar, 106, 264
Malhotra, R. 1993b, Natur, 365, 819
Marzari, F., & Weidenschilling, S. 2002, CeMDA, 82, 225
Masset, F. S., Morbidelli, A., Crida, A., & Ferreira, J. 2006, ApJ, 642, 478
Minton, D. A., & Levison, H. F. 2014, Icar, 232, 118
Morbidelli, A., Bitsch, B., Crida, A., et al. 2016, Icar, 267, 368
Nesvorný, D., & Morbidelli, A. 2012, AJ, 144, 117
Patterson, C. W. 1987, Icar, 70, 319
Quarles, B., & Kaib, N. 2019, AJ, 157, 67
Rafikov, R. R. 2005, ApJL, 621, L69
Storch, N. I., & Batygin, K. 2019, MNRAS, 490, 1861
Wallace, S. C., Boley, A. C., & Quinn, T. 2019, AAS/Division of Dynamical Astronomy Meeting, 51, 302.02
Walsh, K. J., & Levison, H. F. 2016, AJ, 152, 68
Walsh, K. J., Morbidelli, A., Raymond, S. N., O'Brien, D. P., & Mandell, A. M. 2011, Natur, 475, 206
Weidenschilling, S. J. 1977, MNRAS, 180, 57
Weidenschilling, S. J., & Davis, D. R. 1985, Icar, 62, 16
Youdin, A. N. 2010, EAS Publication Ser., 41, 187